



1 **Burn severity and vegetation type control phosphorus** 2 **concentration, molecular composition, and mobilization**

3

4 Morgan E. Barnes¹, J. Alan Roebuck, Jr², Samantha Grieger², Paul J. Aronstein³, Vanessa A.
5 Garayburu-Caruso¹, Kathleen Munson², Robert P. Young¹, Kevin D. Bladon⁴, John D. Bailey⁴,
6 Emily B. Graham^{1,5}, Lupita Renteria¹, Peggy A. O'Day³, Timothy D. Scheibe¹, Allison N.
7 Myers-Pigg^{2,6}

8

9 1 Pacific Northwest National Laboratory, Richland, WA, USA

10 2 Pacific Northwest National Laboratory, Sequim, WA, USA

11 3 Environmental Systems, University of California - Merced, Merced, CA, USA

12 4 College of Forestry, Oregon State University, Corvallis, OR, USA

13 5 School of Biological Sciences, Washington State University, Pullman, WA, USA

14 6 Department of Environmental Sciences, University of Toledo, Toledo, OH, USA

15

16 *Correspondence to:*

17 Allison Myers-Pigg (allison.myers-pigg@pnl.gov)

18 Morgan Barnes (morgan.barnes@pnl.gov)

19

20 Present Addresses:

21 Robert P. Young – Washington River Protection Solutions, P.O. Box 850 MSIN M0-01,
22 Richland, WA 99354

23

24 **Keywords:** char; fire impact; ³¹P NMR; P XANES; sagebrush shrubland; Douglas-fir forest;
25 soil organic matter; nutrient release

26

27 **Abstract**

28 Shifting phosphorus (P) dynamics after wildfires can have cascading impacts from terrestrial to
29 aquatic environments. However, it is unclear if post-fire responses are primarily driven by
30 changes to the molecular composition of the charred material or from the transport of P-
31 containing compounds. We used laboratory leaching experiments of Douglas-fir forest and
32 sagebrush shrubland chars to examine how the potential mobility of P compounds is influenced
33 by different burn severities. Burning produced a 6.9- and 29- fold increase in particulate P
34 mobilization, but a 3.8- and 30.5- fold decrease in aqueous P released for Douglas-fir forest and
35 sagebrush shrubland, respectively. P compound mobilization in the particulate phase was
36 controlled by solid char total P concentrations while the aqueous phase was driven by solubility
37 changes of molecular species. Nuclear magnetic resonance and X-ray absorption near edge
38 structure on the solid chars indicated that organic orthophosphate monoester and diester species
39 were thermally mineralized to inorganic P moieties with burning in both vegetation types. This
40 coincided with the production of calcium- and magnesium-bound inorganic P compounds. With
41 increasing burn severity there were systematic shifts in P concentration and composition—
42 higher severity chars mobilized P compounds in the particulate phase, although the magnitude of
43 change was vegetation specific. Our results indicate a post-fire transformation to both the
44 composition of the solid charred material and to how P compounds are mobilized, which may
45 influence its environmental cycling and fate.



46

47 **Short Summary**

48

49 Wildfires impact nutrient cycles on land and in water. We used burning experiments to
50 understand the types of phosphorous (P), an essential nutrient, that might be released to the
51 environment after different types of fires. We found that the amount of P moving through the
52 environment post-fire is dependent on the type of vegetation and degree of burning which may
53 influence when and where this material is processed or stored.

54

55 **1 Introduction**

56 Wildfires are a major modifier of the terrestrial landscape, directly burning around 4% of the
57 Earth's surface each year (Randerson et al., 2012). They affect both the terrestrial and adjacent
58 aquatic environments and, as such, are considered one of the largest drivers of aquatic
59 impairment (Ball et al., 2021). Organic and inorganic nutrient pools and fluxes can be altered by
60 burning through the loss of volatile compounds, changing physiochemical properties from the
61 incomplete combustion of organic material (from partially charred biomass to ash; collectively
62 referred to as chars (Bird et al., 2015)), and enhancing transport of materials from leaching and
63 erosion (Bodí et al., 2014). Movement of wildfire-derived material from terrestrial landscapes to
64 rivers has impacted 11% of total western United States river length in recent years (Ball et al.,
65 2021). As fire frequency, intensity, severity, and total area burned are expected to increase in
66 many regions, such as the western United States (Doerr and Santín, 2016; Haugo et al., 2019;
67 Jolly et al., 2015), it is important to understand the mechanisms behind how wildfires alter
68 nutrient quantity, composition, and mobilization.

69 Phosphorus (P; occurring primarily as orthophosphate H_2PO_4^- , HPO_4^{2-} , or PO_4^{3-}) is an essential
70 element (Smil, 2000) and is often a limiting nutrient to productivity in terrestrial and aquatic
71 environments (Elser et al., 2007). Ecosystem responses post-fire can include shifting terrestrial
72 nutrient acquisition by decreasing phosphatase activity and promoting net primary production
73 (Dijkstra and Adams, 2015; Saa et al., 1993; Vega et al., 2013). Phosphorus-containing
74 compounds transported to aquatic environments can also increase aquatic productivity,
75 influencing invertebrate and fish size and growth rate (Silins et al., 2014). While there is largely
76 an agreement across studies that P becomes enriched in chars after wildfire (Butler et al., 2018;
77 Elliott et al., 2013; García-Oliva et al., 2018; Schaller et al., 2015), with increased concentrations
78 in mineral soil (Butler et al., 2018) and river systems following wildfire (Lane et al., 2008;
79 Mishra et al., 2021; Rust et al., 2018), we are lacking a systematic understanding on how
80 variable burning conditions mediate the P concentration of charred organic material, and the role
81 of different fire-prone vegetation types (but see (Schaller et al., 2015; Wu et al., 2023b;
82 Yusiharni and Gilkes, 2012)) on availability for mobilization. Prescribed burns and wildfires
83 occur across a range of burning conditions (Merino et al., 2019; Santín et al., 2018; Vega et al.,
84 2013), which results in a mosaic of post-fire ecosystem responses on the landscape (Keeley,
85 2009). Therefore, understanding how P biogeochemistry is altered along a burn gradient will
86 provide insights on heterogenous responses observed across burned landscapes.



87 In the environment, P is found in multiple molecular moieties (i.e., orthophosphate, phosphonate,
88 orthophosphate monoester, orthophosphate diester, polyphosphate; orthophosphate monoester
89 and orthophosphate diester compound classes, referred to as the ester bonds moving forward)
90 which exist in different chemical states (i.e., adsorbed on surfaces, incorporated into minerals,
91 precipitated with metals). Chemical speciation influences the solubility and mobility of P, which
92 in turn impacts its bioavailability (Li and Brett, 2013; Turner et al., 2003b; Weihrauch and Opp,
93 2018; Yan et al., 2023). For example, bonding energy, or strength of the bonds, of the chemical
94 species generally increases from organic P to sorbed and mineral bound P species (Weihrauch
95 and Opp, 2018). The fate of these P species is determined by biological, chemical, physical, and
96 environmental factors, which vary in space and time (Condrón et al., 2015; Yan et al., 2023).
97 Thus, the potential influence of wildfire effects on P dynamics and ecosystem productivity
98 cannot be adequately ascertained by only characterizing P concentration. Compared to changes
99 in total P concentration, there is less understanding of P molecular composition in charred
100 material and the impact this has on its mobilization (Robinson et al., 2018; Wu et al., 2023a). As
101 such, it is unclear if P biogeochemical responses post-fire are due to changing composition of the
102 charred material (i.e., composition controlled) and/or an artifact of how P compounds are
103 transported (i.e., mobilized from the solid char to then be transported through the environment).
104 Recent research on laboratory-produced plant-derived chars has demonstrated the use of NMR to
105 quantify P moiety (Sun et al., 2018; Uchimiya and Hiradate, 2014; Wu et al., 2023b; Xu et al.,
106 2016; Yu et al., 2023) and XANES to identify chemical state (Robinson et al., 2018; Rose et al.,
107 2019; Wu et al., 2023a; Yu et al., 2023). Taken together, these complementary techniques are
108 useful tools to provide a holistic understanding of P molecular composition and can help to
109 determine the environmental fate, as certain compounds are preferentially volatilized, produced,
110 and transported across the landscape (Son et al., 2015).

111 Vegetation burn severity, a common metric to describe how wildfires impact ecosystems, allows
112 for a post-fire assessment of ecosystem impacts (Keeley, 2009). Burn severity is determined by
113 the extent of organic matter loss or change after fire and is influenced by fire intensity, heating
114 duration, degree of live or dead plant material, and fuel moisture, among other factors (Keeley,
115 2009). However, relatively few studies relate burn severity to fire effects on P biogeochemistry
116 (Souza-Alonso et al., 2024; Vega et al., 2013) even though it is a more commonly used field
117 metric than fire intensity because it can be measured after the burn (Zavala et al., 2014). Thus,
118 burn severity allows for understanding how burning conditions beyond temperature influence
119 ecosystems. Experimental studies along burn severity gradients provide an opportunity to better
120 understand field conditions post-fire. To understand the amount and types of materials that could
121 be transported along a burned gradient, we examined how P concentration and molecular
122 composition in solid chars and their leachates vary across a burn severity gradient. We
123 hypothesize that changing P composition in the solid charred materials with increasing burn
124 severity will influence the leachability of P compounds in the particulate and aqueous phases,
125 and this will be moderated by vegetation type. To test this hypothesis and better understand the
126 amount and types of materials that could be mobilized along a burned gradient, we examined
127 how burn severity influences P concentration and molecular composition in experimentally
128 generated solid chars and their leachates.

129

130 **2 Materials and Methods**



131 All datasets and detailed methodology used in this manuscript are available from Grieger et al.
132 (Grieger et al., 2022) version 3 and Barnes et al. (in prep) on the Environmental System Science
133 Data Infrastructure for a Virtual Ecosystem (ESS-DIVE) repository.

134 *2.1 Burn Experiments*

135 Vegetation was collected from two fire-prone landscapes of contrasting vegetation types from
136 the Pacific Northwest, USA that also have differing wildfire characteristics (Roebuck et al.,
137 2024). We represented these landscapes by collecting the dominant vegetation present. In this
138 study, we chose to explore Douglas-fir forests (*Pseudotsuga menziesii*), which tend to burn at
139 higher intensities given fuel loading, and sagebrush shrublands (*Artemisia tridentata*), which
140 tend to burn at lower intensities (Stavi, 2019). In addition, fire exclusion has resulted in Douglas-
141 fir forest encroachment into historically sagebrush shrubland habitat, altering fire dynamics of
142 these landscapes (Everett et al., 2000; Heyerdahl et al., 2006; Strand et al., 2013). Samples were
143 chosen to be representative of possible living vegetation and litter materials of the dominant
144 species from these landscapes. For Douglas-fir, a mix of living and dead material was collected,
145 while sagebrush was in partial senescence upon collection. Woody and canopy materials were
146 mixed at a known ratio before each burn, and this was held constant for each burn (Grieger et al.,
147 2022).

148
149 Chars were generated using an open air burn table, as biochars produced in laboratories have
150 been found to be compositionally different than chars generated in open air burns and wildfires
151 (Myers-Pigg et al., 2024; Santín et al., 2017). To create burns that would result in a range of
152 vegetation burn severities, we manipulated fire behavior on the burn tables by varying burn
153 temperature, duration of heating, fuel moisture content, fuel density, and vegetation status (i.e.,
154 living or litter). Thermocouples were used to monitor temperature over the burn duration, and
155 char grab samples were targeted for 300 °C, 600 °C, and when flames and smoldering
156 commenced (sagebrush shrubland burns did not reach 600 °C). Char burn severity was classified
157 following US Forest Service field metrics based on ash color, degree of consumption, and degree
158 of char (Grieger et al., 2022; Parsons et al., 2010) (Fig. S1). Thus, burn severity was determined
159 by the extent of organic matter loss or change after fire and is influenced by fire intensity,
160 heating duration, degree of live or dead plant material, and fuel moisture, among other factors
161 (Keeley, 2009). Unburned samples and chars were air dried; subsamples were finely ground for
162 elemental composition, and were stored in the dark at room temperature until further analysis.

163 *2.2 Elemental Analysis of Solid Samples*

164 Total P, sulfur (S), aluminum (Al), iron (Fe), magnesium (Mg), calcium (Ca), sodium (Na), and
165 potassium (K) were measured using an inductively coupled plasma optical emission
166 spectrometer (ICP-OES) model Optima 7300 DV (PerkinElmer, Waltham, MA). Solid samples
167 were digested with aqua regia at 130 °C for 8 h in an incubation oven (ThermoFisher Scientific,
168 Waltham, MA).

169 For samples that underwent NMR analysis, approximately 0.5 g of finely ground sample was
170 extracted in a 10 mL solution of 0.25 M NaOH and 0.05 M EDTA for 16 h, followed by
171 centrifugation, filtration, and measurement on ICP-OES (Sun et al., 2018; Turner et al., 2003b).
172 The goal of the NaOH-EDTA extraction is to get the maximum amount of P into solution.
173 Extraction efficiencies are reported in Table S1 (see SI section Method Limitations for additional
174 information).



175 2.3 Solution ^{31}P NMR on Solid Samples

176 After aliquoting 3 mL of the NaOH-EDTA extracts for ICP-OES, the remaining supernatants
177 were frozen and lyophilized to concentrate the extracted compounds. Immediately prior to
178 running NMR experiments (Environmental Molecular Science Laboratory; EMSL, Richland,
179 WA), freeze-dried extracts were reconstituted in 0.52 mL deuterium oxide (D_2O) and 0.26 mL of
180 10 M NaOH, and 0.52 mL of a solution containing 0.5 M NaOH and 0.1 M EDTA. Full
181 experimental ^{31}P NMR measurement details are provided in the supporting information. In brief,
182 NMR measurements were conducted on an Agilent DD2 spectrometer operating at a field
183 strength of 14.1T (242.95 MHz ^{31}P), equipped with a 5mm Varian broadband direct detect probe.
184 Experiments were conducted at a regulated temperature of 20.0°C. A standard 1D pulse and
185 acquire experiment was performed using a 90° pulse width and recycle delay equal to $5 \times T_1$,
186 which were calibrated and measured individually for each sample using the orthophosphate peak
187 present in each. Samples were measured for 16 h each with the number of transients acquired
188 dependent upon T_1 for each individual sample. Post-acquisition processing and analysis was
189 performed using Mnova 14.0.1 (Mestrelab Research, Spain). Details regarding classification of
190 major P forms, identification of specific P compounds from spiking experiments, quantitation,
191 and method limitations are described in detail in the supporting information (Cade-Menun, 2015;
192 Doolette et al., 2009; Recena et al., 2018) (Fig. S2).

193 2.4 Solid Sample P XANES

194 X-ray absorption near edge structure (XANES) is a complementary technique to solution ^{31}P
195 NMR because it can discern the complexation environment of P in solid samples (see SI section
196 Method Limitations for additional information). Bulk XANES was conducted on beamline 14-3
197 at the Stanford Synchrotron Radiation Lightsource (SSRL, Stanford, CA). The beamline was
198 calibrated at the P K-edge with the first peak of tetraphenylphosphonium bromide at 2146.96
199 eV.

200 Sample spectra were fit using least-squares linear combination in Athena (Ravel and Newville,
201 2005) (Fig. S3). Baseline correction and edge-step normalization parameters were varied for
202 individual samples and reference compounds to reduce error (Werner and Prietzel, 2015). Fits
203 were performed with the component sum not forced to unity, a maximum of three reference
204 compounds, and only fits within $\pm 2.5\%$ were used. If a component fit $< 5\%$, then this reference
205 compound was removed, and the sample was refit with the remaining compounds. The R-factor
206 of all sample fits were < 0.05 (Table S2), indicating a good quality of fit (Kelly et al., 2015). Fits
207 were performed with a variety of Ca, Al, Fe, Mn, K, and Na inorganic and organic P-containing
208 reference compounds. Individual inorganic P compounds (P_i ; includes phosphate and
209 pyrophosphate moieties) reference compounds were grouped based on the associated metal and
210 all organic P compounds (P_o ; includes monoester and diester moieties) were kept as a separate
211 category (Fig. S3; Table S3). Additional information on sample preparation, linear combination
212 fits, reference compounds, and method limitations are described in the supplemental information
213 (XANES Methodology section).

214 2.5 Leaching Experiments

215 Leachates from unburned material and char samples were generated in triplicate. Briefly, 25 g of
216 unground sample was shaken in the dark for 24 h in 1000 mL of synthetic rainwater (pH ~ 5) to
217 simulate what might be mobilized by rain events from the solid material and subsequently



218 transported from terrestrial to aquatic environments (Grieger et al., 2022). Our starting mass was
219 kept constant to understand differences in the amounts of materials leached across burn severity
220 gradients, and so our results are directly comparable to temperature gradient studies (Bostick et
221 al., 2018). Therefore, leaching experiments had a different goal of simulating natural
222 mobilization of P compared to the NMR extractions, where we tried to maximize P extracted.
223 Leachates were filtered through a PTFE mesh (2 mm x 0.6 mm) followed by a pre-combusted
224 GF/F filter (< 0.7 μm). Aliquots were immediately taken for subsequent analysis and preserved
225 according to analytical needs described below.

226 2.6 Elemental Analysis of Leachates

227 Coarse filtered (< 2 mm) and < 0.7 μm filtered (i.e., aqueous phase) leachates were preserved in
228 1% nitric acid and stored at 4 °C until analysis. Aliquots of 5 mL were transferred to 15 mL
229 centrifuge tubes, acidified to 10% (v/v) trace metal grade hydrochloric acid and 4% (v/v) trace
230 metal grade nitric acid. Tubes were fully sealed and heated at 85 °C for 2.5 h in an incubation
231 oven (ThermoFisher Scientific, Waltham, MA) and then total elemental analysis were measured
232 by ICP-OES. Total P of the leachate particulate phase (2 mm to 0.7 μm) was calculated as the
233 difference between the coarse filtered and aqueous phase.

234 Molybdate reactive P was determined on aqueous phase leachate aliquots preserved in 0.2%
235 sulfuric acid and stored at 20 °C, following EPA method 365.3 (Method 365.3: Phosphorus, All
236 Forms (Colorimetric, Ascorbic Acid, Two Reagent)). Aqueous non-molybdate reactive P was
237 calculated as the difference between aqueous total P (as measured by ICP-OES) and molybdate
238 reactive P.

239 2.7 Data Analyses

240 Leachable P (mg g⁻¹; particulate and aqueous phases separately) was calculated by normalizing
241 to the P concentration of the solid samples following Equation 1 (Fischer et al., 2023):

$$242 \quad \text{Leachable } P_{\text{particulate or aqueous}} = \frac{\text{leachate } P \text{ (mg L}^{-1}\text{)} \times \text{leaching volume (L)}}{\text{mass of dry char (g)} \times \text{P content of dry char (mg P g}^{-1}\text{)}}$$

243 All statistical tests were conducted in R version 4.2.3 (R Core Team, 2023). Data calculations,
244 statistical analyses, and figures are available on Github ([https://github.com/river-corridors-
245 sfa/rcsfa-RC3-BSLE_P](https://github.com/river-corridors-sfa/rcsfa-RC3-BSLE_P)). For all statistical analyses, model assumptions were assessed with a
246 Shapiro-Wilk test of normality using the package stats (R Core Team, 2023) and spread-location
247 plots to inspect homoscedasticity. All analyses met assumptions after log transformation.
248 Significance was determined at the $\alpha = 0.05$ level. All data are reported as the mean \pm standard
249 deviation unless otherwise stated.

250 Separate analysis of variance (ANOVA) models were used to test how burn severity, vegetation
251 type, and their interaction influences solid P concentration. For leachate samples (i.e., particulate
252 total P, aqueous total P, aqueous molybdate reactive P), mixed-effect models were run with the
253 same fixed effects as the solid samples and a random effect was used to account for triplicate
254 leachates produced from the same solid sample. Mixed effect models were performed with the
255 lme4 package (Bates et al., 2015) and were fit by maximum likelihood. Variance Inflation
256 Factors were used to inspect for multi-collinearity of fixed effects with the car package (Fox and
257 Weisberg, 2018). Post-hoc pairwise comparisons were conducted using least squares means in
258 the emmeans package (Lenth, 2023).



259 Path analysis was conducted to analyze the hypothesized relationships that may explain how
260 burn severity and vegetation type influence P compound mobilization (i.e., leachable particulate
261 or aqueous phase P concentration) indirectly through changes in char conditions (i.e., P
262 concentration and chemical composition). Calcium-bound P_i was used as a proxy for chemical
263 composition because it is a primary control of P compound solubility in charred materials
264 (Schaller et al., 2015; Uchimiya and Hiradate, 2014; Wu et al., 2023b; Yu et al., 2023).
265 Phosphorus compound mobilization was estimated as the average leachable P from the parent
266 solid samples. Models were run with the sem package (Fox, 2006), with burn severity and
267 vegetation type directly impacting the P concentration and proportion of Ca- P_i in the solid
268 samples, which in turn influence the leachable P concentration. Vegetation type is also set up to
269 directly impact burn severity (Fig. S4).

270 **3 Results and Discussion**

271 *3.1 The magnitude of char P increase with burn severity depends on vegetation type*

272 In our study, using experimental open air burns, we found total P concentration increased with
273 burn severity in both Douglas-fir forest and sagebrush shrubland solid samples (Fig. 1). Our
274 findings were consistent with observations of increasing P concentration from laboratory-
275 produced chars (García-Oliva et al., 2018; Zheng et al., 2013) and in chars collected shortly after
276 wildfire and prescribed burns (Butler et al., 2018). The P concentration in unburned Douglas-fir
277 forest samples was 1.3 ± 0.5 g P kg⁻¹ and increased to an average of 6.2 ± 1.9 g P kg⁻¹ in high-
278 severity burns (ANOVA post hoc $p < 0.001$), with temperatures that reached an average of $704 \pm$
279 78 °C. On the other hand, unburned sagebrush shrubland material contained 1.3 g P kg⁻¹
280 compared to 14.5 ± 3.5 g P kg⁻¹ in the moderate-severity burns (ANOVA post hoc $p < 0.001$)
281 that reached 530 ± 25 °C. The observed increase in char P indicated that retention (i.e.,
282 condensation) outweighed loss via volatilization. Generally, P and metal cations volatilize at
283 higher temperatures (>774 °C or greater) than carbon (C) and nitrogen (N) (>200 °C), so they are
284 often retained in charred material rather than lost in gaseous form (Son et al., 2015).



285

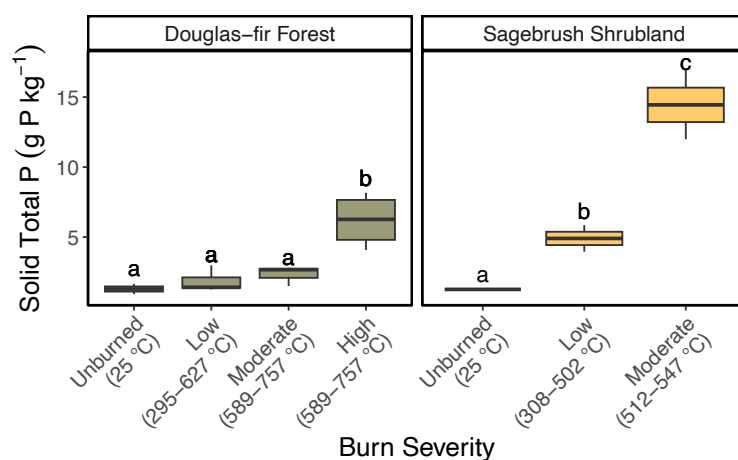


Figure 1. Phosphorus concentration (g P kg^{-1}) in the solid samples along Douglas-fir Forest and Sagebrush shrubland burn severity gradients. Ranges of maximum temperatures ($^{\circ}\text{C}$) reached within a respective burn severity category are reported in parentheses. Letters denote post hoc findings of burn severity significant differences within a vegetation type.

286 Although P concentration in solid samples increased from unburned to the highest severity
287 classification reached in both vegetation types, the magnitude was vegetation dependent
288 (ANOVA interaction term: $F = 6.23$, $p = 0.014$). In Douglas-fir forest chars, P concentration was
289 unchanged by burning until high-severity was reached (post hoc test; low: $p = 0.658$, moderate: $p =$
290 0.277 , high: $p < 0.001$), while P in sagebrush shrubland chars increased even after low-severity
291 burns (post hoc test; low: $p = 0.034$, moderate: $p < 0.001$). Post hoc tests further identified that
292 the P concentration of sagebrush shrubland chars was significantly greater than Douglas-fir
293 forest within the same burn severity classification (low: $p = 0.0038$; moderate: $p < 0.001$), even
294 though unburned samples were not statistically different ($p = 0.962$). On average, total P in
295 sagebrush shrubland chars were 2.7 and 6.2 times higher than Douglas-fir forest in low and
296 moderate-severity burns, respectively (Fig. 1).

297 Remarkably, P in moderate-severity sagebrush shrubland chars was even higher than Douglas-fir
298 forest high-severity chars. Higher maximum char temperatures or burn duration does not explain
299 why P concentration is greater in burned sagebrush shrubland material compared to Douglas-fir
300 forest; sagebrush shrublands experienced lower temperatures (530 ± 25 $^{\circ}\text{C}$) and burn duration
301 (202 ± 3 minutes) in moderate-severity burns compared to Douglas-fir forest high-severity burns
302 (704 ± 78 $^{\circ}\text{C}$; 783 ± 195 minutes; Table S4).

303 One mechanism that could explain such results is that sagebrush shrublands may be composed of
304 volatile compounds that are more susceptible to loss compared to Douglas-fir forests, leading to
305 selective enrichment of P compounds relative to Douglas-fir forest chars. However, emission
306 factors and total volatile organic compounds from sagebrush and coniferous fuels are relatively
307 similar (Hatch et al., 2019; McMeeking et al., 2009). This suggests that the observed enrichment



308 of sagebrush shrubland P with burning may be due to differences in how specific P compounds
309 in the sagebrush shrubland materials are retained compared to other compounds that are
310 combusted efficiently in those chars, which can arise from different fire conditions (Fiddler et
311 al., 2024). Sagebrush shrublands may be more susceptible to changing P dynamics post-fire
312 because chars are likely enriched in P to a greater extent than Douglas-fir forests, even at low
313 severities.

314 *3.2 Solid char molecular composition is influenced by burn severity and vegetation type*

315 Organic P in the solid char was progressively transformed to inorganic species across both
316 vegetation types. Unburned Douglas-fir forest and sagebrush shrubland had similar initial
317 percentages of total organic P with $40.5 \pm 3.3\%$ and 53.7% , respectively (identified by NMR
318 extracts, Fig. 2; also supported by XANES on solid phase, Fig. 3). As burning progressed, the
319 total organic P pools reduced to only $12.6 \pm 8.2\%$ for Douglas-fir forest and $10.4 \pm 8.4\%$ for
320 sagebrush shrubland low-severity chars. While organic P moieties were still present in Douglas-
321 fir forest chars produced at moderate severities ($4.4 \pm 4.2\%$), $<1\%$ was measured in sagebrush
322 shrubland. Moderate-severity sagebrush shrubland chars more closely resembled high-severity
323 Douglas-fir forest with nearly all organic P moieties lost ($<1\%$). This further supports the
324 conclusion that different fire conditions were experienced by Douglas-fir forest and sagebrush
325 shrubland in our simulated burns. Although it has been suggested that organic P can be fully
326 transformed to inorganic species at $200\text{ }^{\circ}\text{C}$ (García-Oliva et al., 2018), another study of organic
327 horizons found organic P moieties persisted after low, moderate, and high-severity fires that
328 reached up to $872\text{ }^{\circ}\text{C}$ (Merino et al., 2019). We measured organic P in burns that reached above
329 $600\text{ }^{\circ}\text{C}$, suggesting that the thermal mineralization of organic to inorganic P compounds is
330 controlled by microscale differences in temperature and selective protection rather than what is
331 observed at overall bulk temperatures, and is likely a result of the interaction between
332 temperature, burn duration, and vegetation type experienced by these microsites (Galang et al.,
333 2010; Lopez et al., 2024).



334

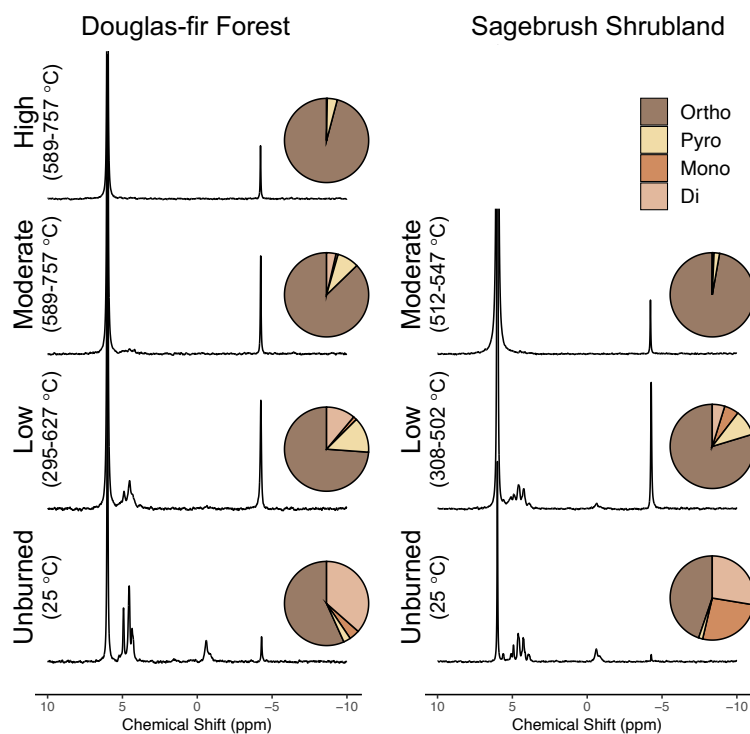


Figure 2. Solution ^{31}P nuclear magnetic resonance (NMR) spectra from a representative solid char sample of each burn severity and vegetation type. The number of scans varied for each sample, based on relaxation time, and therefore direct comparisons of peak intensities can only be made within a spectrum (see additional details in SI NMR Methods). Averaged replicates are represented by pie charts for the proportions of orthophosphate (ortho), pyrophosphate (pyro) monoesters (mono) and diesters (di). Orthophosphate and pyrophosphate are inorganic species (brown colors) and monoester and diesters are organic species (orange colors). Ranges of maximum temperatures ($^{\circ}\text{C}$) reached within a respective burn severity category are reported in parentheses. See SI sections NMR Methodology and Method Limitations for additional details.

335

336 Previous studies have suggested charred materials containing diester species (two C moieties per
337 P) are more vulnerable to thermal mineralization than monoesters (one C moiety per P) (García-
338 Oliva et al., 2018; Turrion et al., 2010). However, we found diester and monoester species
339 followed similar proportional decreases in our chars with burning (Fig. S5). Hence, both readily
340 available (i.e., diester) and less labile (i.e., monoester) organic P species (Condon et al., 2015)
341 were converted to inorganic P at comparable rates, which is similar to forest and shrubland



342 organic horizons subjected to prescribed fire (Merino et al., 2019). This suggests there is not a
343 fundamental molecular difference in how these moieties respond to burning in organic material,
344 but instead the preferential loss of diesters in burned mineral soil may be because the stronger
345 sorption of monoesters to soil particles attenuates the heat.

346 Because diester and monoester species were lost at similar proportions, the composition of the
347 unburned material dictated the resulting char P composition and potential bioavailability. Across
348 both vegetation types, we identified phospholipids, DNA, and RNA (diester region) and phytate
349 and sugar phosphates (monoester region; Fig. 2; Table S5), which follows other studies of
350 vegetation P composition (Doolette and Smernik, 2016; Noack et al., 2012). However, the
351 proportions of these species were vegetation dependent, where unburned Douglas-fir forest was
352 dominated by diesters ($36.5 \pm 9.1\%$) with minor percentages of monoesters ($4.1 \pm 5.7\%$),
353 whereas sagebrush shrubland was nearly equal parts diesters (27.6%) and monoesters (26.1%).
354 RNA, DNA, phospholipids, and sugar phosphates are considered bioavailable due to their weak
355 adsorption, whereas phytate strongly sorbs to both organic and inorganic particles making it
356 relatively less available for biological uptake (Condrón et al., 2015; Li and Brett, 2013; Turner et
357 al., 2003a). Douglas-fir forest was composed of a greater proportion of these bioavailable
358 organic species in unburned ($36.8 \pm 7.6\%$) and low-severity burns ($12.4 \pm 8.4\%$) compared to
359 sagebrush shrubland (unburned: 32.4; low: $8.0 \pm 4.5\%$).

360 With increased burn severity, Douglas-fir forest (high-severity) and sagebrush shrubland
361 (moderate-severity) organic speciation converged with only $< 1\%$ of organic P (as RNA)
362 remaining. Prior studies using NMR in plant-based biochar produced from 300 – 800 °C found
363 char was composed of entirely inorganic P, including orthophosphate (27–97%) and
364 pyrophosphate (3–71%; although one sample produced at 350 °C was 2% phospholipids) (Sun et
365 al., 2018; Uchimiya et al., 2015; Uchimiya and Hiradate, 2014). The unburned parent material in
366 these studies had variable starting compositions with organic P ranging from 3–87% (as phytate).
367 The extent of organic P loss in these studies is most similar to our higher severity samples, once
368 again demonstrating that more than temperature determines the composition of P in charred
369 material. Overall, these findings suggest organic P moieties in charred material are determined by
370 the degree of burning, where lower severity chars resemble the starting composition, and this is
371 influenced by vegetation type.

372 As organic species were thermally mineralized in our chars, inorganic P, such as pyrophosphate,
373 was produced (Fig. 2). Pyrophosphate is thought to largely originate from fungal tissue
374 (Bünemann et al., 2008; Makarov et al., 2005), and it has been found in some plants (Noack et
375 al., 2012; Wu et al., 2023b). We found pyrophosphate peaked in low-severity chars across both
376 vegetation types, reaching $13.6 \pm 3.1\%$ in Douglas-fir forest and $9.9 \pm 6.2\%$ in sagebrush
377 shrubland burns. Prior NMR studies on plant chars produced between 350 - 800 °C have also
378 observed an increase in the proportion of pyrophosphate relative to unburned material, followed
379 by a decrease at higher charring conditions (Sun et al., 2018; Uchimiya and Hiradate, 2014).
380 Variability in pyrophosphate from naturally produced chars has also been observed. For
381 example, post wildfire, pyrophosphate was $\sim 3\%$ in a pine forest (García-Oliva et al., 2018),
382 absent in a eucalyptus forest (Santín et al., 2018), 0–13% of cedar-hemlock forests (Cade-Menun
383 et al., 2000), and 3–7% from pine forests and shrublands (Merino et al., 2019). Thus burned
384 organic material, especially in chars produced at low-severity wildfire and prescribed burns, may
385 be an important, yet underappreciated, source of pyrophosphate in the environment.



386 The production of pyrophosphate in our charred plant material is likely a result of the initial
387 organic matter composition and burning conditions (Wu et al., 2023b; Yu et al., 2023).
388 Pyrophosphate and other polyphosphates can be produced from orthophosphate during burning,
389 with the thermal degradation of phytate (organic P; monoester) contributing more
390 orthophosphate (Robinson et al., 2018; Rose et al., 2019; Uchimiya and Hiradate, 2014).
391 Pyrophosphate was greater in Douglas-fir forest chars compared to sagebrush shrublands, even
392 though sagebrush shrubland chars contained more phytate in the unburned material (Fig. 2). This
393 indicates pyrophosphate was primarily produced from polymerization and dehydration of
394 orthophosphate, and not from thermal degradation of phytate in our chars (Uchimiya and
395 Hiradate, 2014).

396 Although pyrophosphate peaked in low-severity chars, we found the percentage of total
397 inorganic P species continued to increase with burning across both vegetation types, as measured
398 by NMR on solid extracts and XANES of intact solid samples (Fig. 2, Fig. 3; Tables S2 and S5),
399 demonstrating additional transformations to P composition with increasing severity. Inorganic
400 species, measured by XANES, in unburned material was composed largely of P compounds
401 associated with Fe (37% sagebrush shrubland; $40 \pm 5\%$ Douglas-fir forest; fitting primarily as P_i
402 sorbed to the surface of goethite) and a minor component of Ca-bound P_i species ($3 \pm 3\%$
403 Douglas-fir forest; 9% sagebrush shrubland; fitting mostly as apatite). The proportion of Ca- and
404 Mg- P_i (fitting as magnesium phosphate and/or struvite) increased with burn severity (Fig. 3;
405 Table S2). Douglas-fir forest high-severity chars had $52.8 \pm 8.3\%$ Ca- P_i and $29.0 \pm 9.9\%$ Mg- P_i ,
406 while sagebrush shrubland moderate-severity chars contained $45.1 \pm 0.1\%$ Ca- P_i and $53.7 \pm$
407 0.1% Mg- P_i .

408 Other studies using XANES supports the production of Ca- P_i , along with Fe- or Mg- P_i in plant-
409 based chars and ash (Robinson et al., 2018; Sun et al., 2018; Uchimiya and Hiradate, 2014; Wu
410 et al., 2023a), whereas studies using other techniques (solid-state NMR, sequential fractionation)
411 have found higher temperatures result in greater Ca- and Al- P_i (García-Oliva et al., 2018; Xu et
412 al., 2016). Hydroxyapatite and other stable forms of Ca- P_i minerals are known to be produced by
413 organic matter combustion (Uchimiya and Hiradate, 2014), so it follows that these P species are
414 produced with burning and progressively increase along our burn severity gradient. P compound
415 bonding environments have been found to resemble stoichiometric ratios of the burned material
416 (Wu et al., 2023a; Zwetsloot et al., 2015). Our findings support this where Ca- and Mg- P_i species
417 increased as the proportion of Ca and Mg also increased (Fig. 3; Tables S2, S6, and S7).
418 Phosphorus mobility and bioavailability of P compounds are likely influenced by increased
419 inorganic P proportions because Ca- P_i , especially apatite, is considered to have low water
420 extractability and apparent bioavailability (García-Oliva et al., 2018; Li and Brett, 2013;
421 Zwetsloot et al., 2015).



422

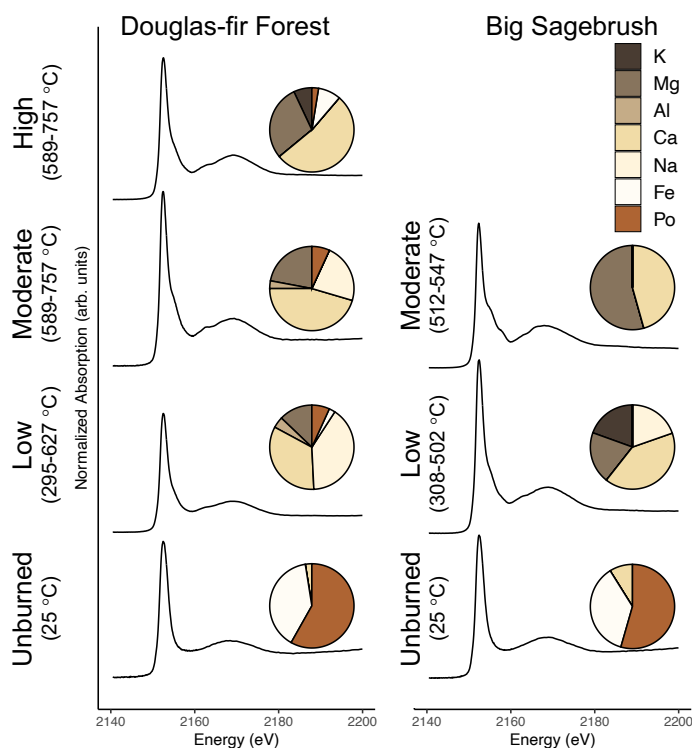


Figure 3. Phosphorus K-edge X-ray absorption near edge structure (XANES) spectroscopy from a representative solid unburned and char sample of each burn severity and vegetation type. Averaged replicates are represented by pie charts for the proportions of P_i associated with K-, Mg-, Al-, Ca-, Na-, and Fe (brown colors) and P_o species grouped together regardless of metal association (orange color; see SI XANES Methods for additional details). Ranges of maximum temperatures ($^{\circ}\text{C}$) reached within a respective burn severity category are reported in parentheses. See SI sections XANES Methodology and Method Limitations for additional details.

423

424 *3.3 Leachable particulate- and aqueous-bound P have contrasting mobilization patterns with*
425 *burning and are under differing controls*

426 As burn severity increased, the enriched P of the solid chars resulted in greater particulate P
427 mobilized (assessed via leaching experiments), regardless of vegetation type ($\beta = 0.78$, $p <$
428 0.001 , $r^2 = 0.68$; Fig. 4, Fig. 5). Burning resulted in a 6.9- and 29- fold increase of particulate P
429 mobilization from Douglas-fir forest (high-severity) and sagebrush shrubland (moderate-
430 severity) chars, respectively (Fig. 4). Phosphorus compounds may be largely physically protected
431 in the matrix of the charred material (70–90% residual P in sequential fractionation scheme (Wu



432 et al., 2023b)), therefore it follows that particulate P patterns are controlled by changes in solid
433 char concentration; charred material becomes enriched with P and there is production of highly
434 mobile particulates (such as ash (Blake et al., 2010)). Path analysis identified that burn severity
435 ($\beta = 0.61, p < 0.001$) and vegetation type ($\beta = 0.65, p < 0.001$) had direct influence on solid char
436 P concentration ($r^2 = 0.64$; Fig. 5). Mixed effect model results further demonstrate that the effect
437 burn severity has on leachable particulate P is vegetation dependent (interaction term of mixed
438 effect model; $p = 0.009$). Moderate-severity sagebrush shrubland chars mobilized 5.2 times more
439 P in the particulate phase than Douglas-fir forest ($p = 0.04$). Particulate P mobilized from charred
440 material can be transported to waterways, as a meta-analysis found unfiltered P concentrations in
441 the western United States increased ~ 1.7 times after wildfire ($n = 46$) (Rust et al., 2018).

442 In contrast to leachable particulate P, mobilization of P in the aqueous phase decreased 3.8-fold
443 for Douglas-fir forest and 30.5-fold for sagebrush shrubland with burning (Fig. 4). Instead of
444 concentration-controlled like particulate P, aqueous P mobilization was composition-controlled,
445 represented as percentage of Ca-P_i in our path analysis ($\beta = -0.44, p = 0.041, r^2 = 0.34$; Fig. 5).
446 Prior work from laboratory-produced plant chars have also found decreased water-soluble P even
447 though solid char concentration increased with burning (Gundale and DeLuca, 2006; Mukherjee
448 and Zimmerman, 2013; Wu et al., 2011; Yu et al., 2023; Zheng et al., 2013). Phosphorus
449 compound adsorption to multivalent cations (Ca^{2+} , Mg^{2+} , Fe^{3+} , and Al^{3+}) can decrease aqueous
450 phase export (Glaser et al., 2002). Indeed, we found higher severity burns had greater
451 concentrations of metals (Tables S6 and S7) which interacted with P to form primarily Ca- and
452 Mg-P_i species (Fig. 3; Table S2).



453

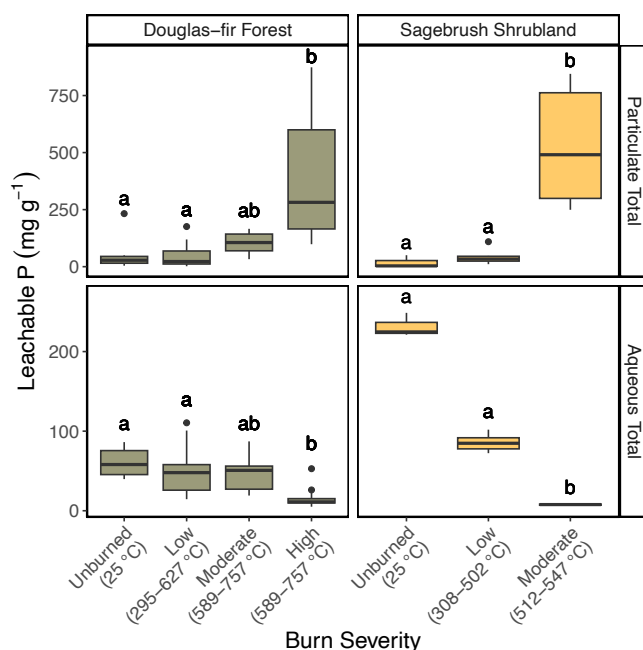


Figure 4. Relationship of burn severity and vegetation type with leachable P concentration (mg P g^{-1} ; calculated from Equation 1) for total P in the particulate phase and total P in the aqueous phase. Molybdate-reactive P in the aqueous phase are reported in the SI. Ranges of maximum temperatures ($^{\circ}\text{C}$) reached within a respective burn severity category are reported in parentheses. Letters denote post hoc findings of burn severity significant differences within a vegetation type. Note difference scales of the y-axis for the particulate and aqueous phases. See Figure S6 for leachable aqueous molybdate reactive P results.

454

455 Additional changes to char composition, including organic P speciation and pH, also likely
456 contributed to decreased aqueous P mobilization with increased burning. We found a decrease in
457 non-molybdate reactive aqueous P, which is largely composed of organic P species (Condon et
458 al., 2015), with increasing burn severity (mixed effect model interaction term: $p < 0.001$, Fig. S6)
459 indicating less mobilization of organic P species with burning. The amount of mobilized P
460 compounds from char is also related to pH, where less P compounds are released at higher pH
461 (Silber et al., 2010; Zheng et al., 2013). We found aqueous P mobilization had an inverse
462 relationship with pH for both Douglas-fir forest ($p < 0.001$; $r^2 = 0.45$) and sagebrush shrubland
463 ($p < 0.001$, $r^2 = 0.97$; Fig. S7). Overall, changing chemical composition of the charred material
464 decreases solubility and therefore reduces aqueous P mobilization into the environment
465 (Robinson et al., 2018; Uchimiya et al., 2015; Wu et al., 2023b; Xu et al., 2016).



466 The extent of decreased aqueous P mobilization was vegetation dependent (interaction term of
 467 mixed effect model; $p < 0.001$; Fig. 4). However, because both vegetation types had similar
 468 percentages of Ca-P_i ($p = 0.18$; $r^2 = 0.15$), it indicates additional controls on aqueous P
 469 mobilization. In addition to Ca-P_i and Mg-P_i, moderate-severity Douglas-fir forest contained P
 470 compounds associated with Na (XANES: $22.7 \pm 22.1\%$) and organic P species (XANES: $6.9 \pm$
 471 11.9% ; NMR: $4.4 \pm 4.2\%$), whereas sagebrush shrubland was $<1\%$ organic P (XANES: $0 \pm 0\%$;
 472 NMR: $0.7 \pm 0.4\%$; Fig.s 2 and 3; Tables S2 and S5). Greater solubility of these chemical species
 473 likely contributes to Douglas-fir forest moderate-severity burns mobilizing 6.4 times more
 474 aqueous P than sagebrush shrubland ($p = 0.004$). Changing chemical speciation from soluble
 475 organic P to less soluble inorganic species (Mukherjee and Zimmerman, 2013; Xu et al., 2016)
 476 resulted in the decreased export of P compounds with increased burn severity and contributed to
 477 the amount of P compounds mobilized from the respective vegetation types. This has important
 478 implications for P compounds are transported in the environment because organic P can leach
 479 faster than inorganic (McDowell et al., 2021).

480

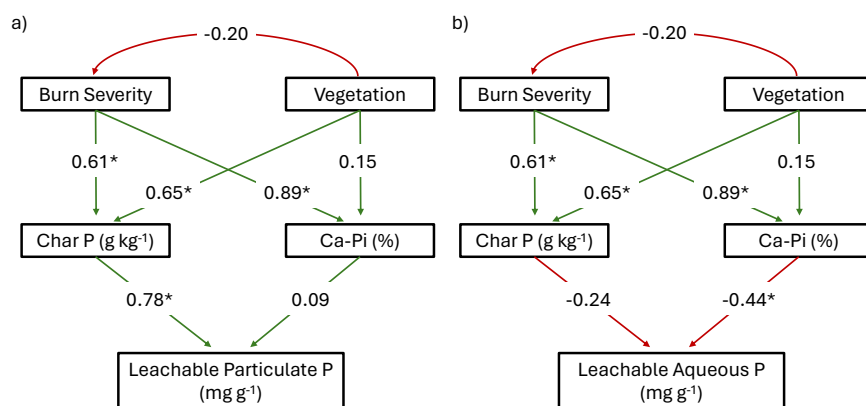


Figure 5. Path analysis model results for the impact of burn severity and vegetation type on leachable P in the (a) particulate and (b) aqueous phases, as mediated by solid unburn and char P concentration and chemical composition. All relationships are reported with significance ($\alpha = 0.05$) denoted with an asterisk symbol on the standardized correlation coefficient (analogous to relative regression weights). Paths are green for positive relationships and red for negative. Leachable Particulate P Model: $\chi^2 = 16.277$, $p < 0.05$, $df = 3$, RMSEA = 0.483, AIC = 108.3; Leachable Aqueous P Model: $\chi^2 = 19.032$, $p < 0.05$, $df = 3$, RMSEA = 0.530, AIC = 122.1. See Fig S4 for original hypothesized model.

481

482 4 Conclusions

483 Our objective was to understand how P concentration and composition of charred vegetation
 484 changes along burned gradients to then influence the amount of P potentially mobilized into the
 485 environment. We found systematic changes in P chemistry across vegetation types and
 486 summarize these findings into a conceptual model (Fig. 6). Identifiable structures decreased with
 487 increasing black charring and/or white ash with increasing burn severity. Total Ca, Fe, Al, K,
 488 Ma, and Na concentrations increased while total C was lost as charring occurred. Solid char



489 concentration and composition controlled how P compounds were mobilized from burned
490 material. Overall, burning resulted in an increase of char P concentration, which subsequently
491 controlled the mobilization of particulate-bound P compounds from the chars. As burning
492 progressed, chars compositionally transitioned from proportionally more organic P species,
493 including both monoester and diesters, to Ca- and Mg- bound inorganic P species. These
494 compositional changes resulted in less soluble inorganic P species and therefore reduced aqueous
495 P mobilization in higher severity burns. Across vegetation types, chars became more divergent
496 from the unburned vegetation material in P composition and mobilization potential as burning
497 continued. Burn severity and vegetation type indirectly influenced the quantity and leachable
498 phase (i.e., particulate or aqueous) of P compounds that were mobilized from charred material by
499 altering solid sample concentration and composition.

500 Although both vegetation types followed similar concentration and compositional patterns,
501 sagebrush shrubland tended to appear ‘more burned’ than Douglas-fir forest in our P burn
502 severity conceptual model (Fig. 6). The P concentration of Douglas-fir forest chars and leachates
503 were more resilient to change with burning compared to sagebrush shrubland. For example,
504 generally, P transformations in sagebrush shrubland moderate-severity burns chemically
505 resembled that of Douglas-fir forest high-severity burns. Taken together, this indicates that
506 although sagebrush shrubland experiences more low- and moderate-severity burns (Stavi, 2019),
507 the response of P chemistry post-fire may resemble Douglas-fir forests burned at higher
508 severities. This response is important to note as shifts in fire severity are not occurring uniformly
509 across all ecosystem type (Francis et al., 2023; Halofsky et al., 2020; Reilly et al., 2017).

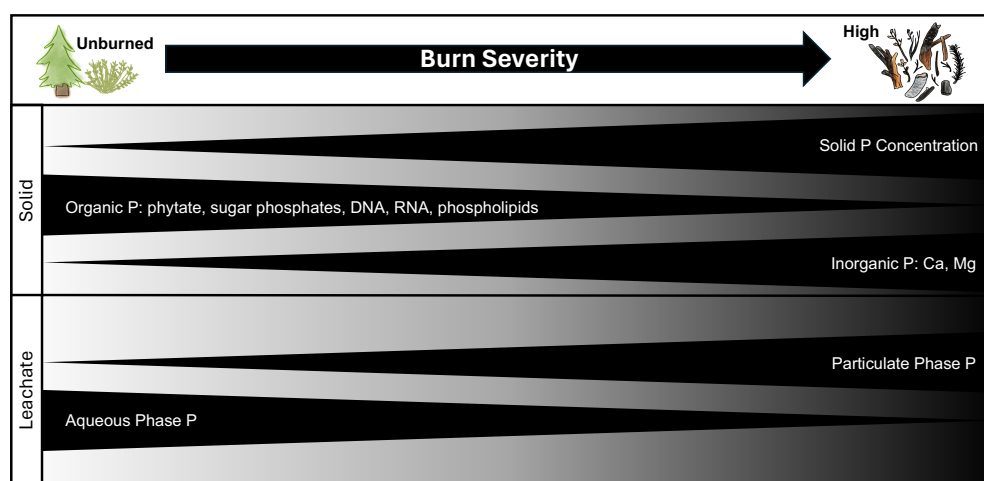


Figure 6. Conceptual framework for phosphorus biogeochemical shifts with increasing burn severity where solid P concentration increases, organic P species decrease while inorganic P increases. Leachates from the solid samples increased in mobilization of P in the particulate phase but decreased in aqueous P with burning.



511 Organic soil horizons immobilize large amounts of P (Kruse et al., 2015) that can then serve as
512 an important source of bioavailable P after burning (Schaller et al., 2015). The key to
513 bioavailable P is that it can enter solution for subsequent uptake by plants and microbes (Kruse et
514 al., 2015). Our leaching experiments provide insight to the potential mobilization, and therefore
515 bioavailability, of P from solid vegetation chars. We found burning resulted in less P released
516 into the environment in the aqueous phase, although particulate-bound P increased and may be
517 an important source of available over longer timeframes. Our study helps to provide additional
518 information on the potential environmental fate of P post-fire in the context of different burn
519 severities and ecosystem types.

520 **Acknowledgments**

521 We thank Christopher Myers for assistance with the ICP analyses and Sophia McKeever for help
522 with measuring molybdate reactive P. This research was supported by the U.S. Department of
523 Energy, Office of Science, Office of Biological and Environmental Research, Environmental
524 System Science (ESS) Program. This contribution originates from the River Corridor Scientific
525 Focus Area project at Pacific Northwest National Laboratory (PNNL). PNNL is operated by
526 Battelle Memorial Institute for the United States Department of Energy under contract no. DE-
527 AC05-76RL01830. Portions of this research were performed on a project award
528 ([10.46936/lser.proj.2021.51840/60000342](https://www.osti.gov/proj/2021.51840/60000342)) from the Environmental Molecular Science
529 Laboratory (EMSL) (grid.436923.9), a DOE Office of Science User Facility sponsored by the
530 Biological and Environmental Research program under Contract No. DE-AC05-76RL01830.
531 XANES data were collected from the Stanford Synchrotron Radiation Lightsource, SLAC
532 National Accelerator Laboratory, which is supported by the U.S. Department of Energy, Office
533 of Science, Office of Basic Energy Sciences under Contract No. DE-AC02-76SF00515. We
534 would like to give a special thanks to Erik Nelson, the beamline scientist from SSRL that helped
535 us collect those data.

536 **Code/Data availability**

537 All data and code are publicly available on the Environmental System Science Data
538 Infrastructure for a Virtual Ecosystem (ESS-DIVE) repository (Grieger et al., 2022) or GitHub
539 (https://github.com/river-corridors-sfa/resfa-RC3-BSLE_P).

540

541 **Competing interests**

542 The authors declare no competing interests.

543

544 **Author Contribution**

545 Conceptualization: M.E.B., A.N.M.-P., J.A.R., K.D.B., E.B.G., S.G., T.D.S. Methodology and
546 Software: A.N.M.-P., M.E.B., S.G., J.D.B., K.B., E.B.G., P.A., V.A.G.-C., K.M., J.A.R., R.P.Y.,
547 P.A.O., L.R. Investigation: M.E.B., P.A., S.G., K.M., L.R., J.A.R., J.D.B., K.D.B., R.P.Y. Data
548 Curation: M.E.B., S.G., P.A., V.A.G.-C., A.N.M.-P., K.M., J.D.B., K.D.B., L.R., J.A.R. Formal
549 Analysis: M.E.B., A.N.M.-P., J.A.R., V.A.G.-C., P.A., P.A.O., R.P.Y. Validation: M.E.B., P.A.,
550 K.M., V.A.G.-C., A.N.M.-P., P.A.O., R.P.Y. Visualization: M.E.B., A.N.M.-P., S.G. Writing -



551 Original Draft: M.E.B., A.N.M.-P., J.A.R., S.G., K.M., R.P.Y. Writing – Review and Editing:
552 M.E.B., P.A., J.D.B., K.D.B., V.A.G.-C., E.B.G., A.N.M.-P., P.A.O., L.R., J.A.R., T.D.S., R.P.Y.

553

554 **References**

555 Ball, G., Regier, P., González-Pinzón, R., Reale, J., and Van Horn, D.: Wildfires increasingly
556 impact western US fluvial networks, *Nat. Commun.*, 12, 2484, 2021.

557 Bates, D., Mächler, M., Bolker, B., and Walker, S.: Fitting Linear Mixed-Effects Models Using
558 lme4, *J. Stat. Softw.*, 67, 1–48, 2015.

559 Bird, M. I., Wynn, J. G., Saiz, G., Wurster, C. M., and McBeath, A.: The pyrogenic carbon
560 cycle, *Annu. Rev. Earth Planet. Sci.*, 43, 273–298, 2015.

561 Blake, W. H., Theocharopoulos, S. P., Skoulikidis, N., Clark, P., Tountas, P., Hartley, R., and
562 Amaxidis, Y.: Wildfire impacts on hillslope sediment and phosphorus yields, *J. Soils Sediments*,
563 10, 671–682, 2010.

564 Bodí, M. B., Martin, D. A., Balfour, V. N., Santín, C., Doerr, S. H., Pereira, P., Cerdà, A., and
565 Mataix-Solera, J.: Wildland fire ash: Production, composition and eco-hydro-geomorphic effects,
566 *Earth-Sci. Rev.*, 130, 103–127, 2014.

567 Bostick, K. W., Zimmerman, A. R., Wozniak, A. S., Mitra, S., and Hatcher, P. G.: Production
568 and Composition of Pyrogenic Dissolved Organic Matter From a Logical Series of Laboratory-
569 Generated Chars, *Frontiers in Earth Science*, 6, 43, 2018.

570 Bünemann, E. K., Smernik, R. J., Marschner, P., and McNeill, A. M.: Microbial synthesis of
571 organic and condensed forms of phosphorus in acid and calcareous soils, *Soil Biol. Biochem.*,
572 40, 932–946, 2008.

573 Butler, O. M., Elser, J. J., Lewis, T., Mackey, B., and Chen, C.: The phosphorus-rich signature of
574 fire in the soil-plant system: a global meta-analysis, *Ecol. Lett.*, 21, 335–344, 2018.

575 Cade-Menun, B. J.: Improved peak identification in ³¹P-NMR spectra of environmental samples
576 with a standardized method and peak library, *Geoderma*, 257–258, 102–114, 2015.

577 Cade-Menun, B. J., Berch, S. M., Preston, C. M., and Lavkulich, L. M.: Phosphorus forms and
578 related soil chemistry of Podzolic soils on northern Vancouver Island. II. The effects of clear-
579 cutting and burning, *Can. J. For. Res.*, 30, 1726–1741, 2000.

580 Condon, L. M., Turner, B. L., and Cade-Menun, B. J.: Chemistry and dynamics of soil organic
581 phosphorus, in: *Phosphorus: Agriculture and the Environment*, American Society of Agronomy,
582 Crop Science Society of America, and Soil Science Society of America, Madison, WI, USA, 87–
583 121, 2015.

584 Dijkstra, F. A. and Adams, M. A.: Fire Eases Imbalances of Nitrogen and Phosphorus in Woody
585 Plants, *Ecosystems*, 18, 769–779, 2015.



- 586 Doerr, S. H. and Santín, C.: Global trends in wildfire and its impacts: perceptions versus realities
587 in a changing world, *Philos. Trans. R. Soc. Lond. B Biol. Sci.*, 371,
588 <https://doi.org/10.1098/rstb.2015.0345>, 2016.
- 589 Doolette, A. L. and Smernik, R. J.: Phosphorus speciation of dormant grapevine (*Vitis vinifera*L.)
590 canes in the Barossa Valley, South Australia, *Aust. J. Grape Wine Res.*, 22, 462–468, 2016.
- 591 Doolette, A. L., Smernik, R. J., and Dougherty, W. J.: Spiking improved solution phosphorus-31
592 nuclear magnetic resonance identification of soil phosphorus compounds, *Soil Sci. Soc. Am. J.*,
593 73, 919–927, 2009.
- 594 Elliott, K. J., Knoepp, J. D., Vose, J. M., and Jackson, W. A.: Interacting effects of wildfire
595 severity and liming on nutrient cycling in a southern Appalachian wilderness area, *Plant Soil*,
596 366, 165–183, 2013.
- 597 Elser, J. J., Bracken, M. E. S., Cleland, E. E., Gruner, D. S., Harpole, W. S., Hillebrand, H.,
598 Ngai, J. T., Seabloom, E. W., Shurin, J. B., and Smith, J. E.: Global analysis of nitrogen and
599 phosphorus limitation of primary producers in freshwater, marine and terrestrial ecosystems,
600 *Ecol. Lett.*, 10, 1135–1142, 2007.
- 601 Everett, R. L., Schellhaas, R., Keenum, D., Spurbeck, D., and Ohlson, P.: Fire history in the
602 ponderosa pine/Douglas-fir forests on the east slope of the Washington Cascades, *For. Ecol.*
603 *Manage.*, 129, 207–225, 2000.
- 604 Fiddler, M. N., Thompson, C., Pokhrel, R. P., Majluf, F., Canagaratna, M., Fortner, E. C.,
605 Daube, C., Roscioli, J. R., Yacovitch, T. I., Herndon, S. C., and Bililign, S.: Emission factors
606 from wildfires in the Western US: An investigation of burning state, ground versus air, and
607 diurnal dependencies during the FIREX-AQ 2019 campaign, *J. Geophys. Res.*, 129,
608 <https://doi.org/10.1029/2022jd038460>, 2024.
- 609 Fischer, S. J., Feghel, T. S., Wilkerson, P. J., Rivera, L., Rhoades, C. C., and Rosario-Ortiz, F. L.:
610 Fluorescence and Absorbance Indices for Dissolved Organic Matter from Wildfire Ash and
611 Burned Watersheds, *ACS EST Water*, 3, 2199–2209, 2023.
- 612 Fox, J.: TEACHER’S CORNER: Structural Equation Modeling With the sem Package in R,
613 *Struct. Equ. Modeling*, 13, 465–486, 2006.
- 614 Fox, J. and Weisberg, S.: *An R Companion to Applied Regression*, SAGE Publications, 608 pp.,
615 2018.
- 616 Francis, E. J., Pourmohammadi, P., Steel, Z. L., Collins, B. M., and Hurteau, M. D.: Proportion
617 of forest area burned at high-severity increases with increasing forest cover and connectivity in
618 western US watersheds, *Landsc. Ecol.*, 38, 2501–2518, 2023.
- 619 Galang, M. A., Markewitz, D., and Morris, L. A.: Soil phosphorus transformations under forest
620 burning and laboratory heat treatments, *Geoderma*, 155, 401–408, 2010.



- 621 García-Oliva, F., Merino, A., Fonturbel, M. T., Omil, B., Fernández, C., and Vega, J. A.: Severe
622 wildfire hinders renewal of soil P pools by thermal mineralization of organic P in forest soil:
623 Analysis by sequential extraction and ³¹P NMR spectroscopy, *Geoderma*, 309, 32–40, 2018.
- 624 Glaser, B., Lehmann, J., and Zech, W.: Ameliorating physical and chemical properties of highly
625 weathered soils in the tropics with charcoal – a review, *Biol. Fertil. Soils*, 35, 219–230, 2002.
- 626 Grieger, S., Bailey, J., Barnes, M., Bladon, K. D., Forbes, B., Garayburu-Caruso, V. A., Graham,
627 E. B., Goldman, A. E., Homolka, K., McKeever, S. A., Myers-Pigg, A., Otenburg, O., Renteria,
628 L., Roebuck, A., Scheibe, T. D., and Torgeson, J. M.: Organic Matter Concentration and
629 Composition of Experimentally Burned Open Air and Muffle Furnace Vegetation Chars across
630 Differing Burn Severity and Feedstock Types from Pacific Northwest, USA (V3),
631 <https://doi.org/10.15485/1894135>, 2022.
- 632 Gundale, M. J. and DeLuca, T. H.: Temperature and source material influence ecological
633 attributes of ponderosa pine and Douglas-fir charcoal, *For. Ecol. Manage.*, 231, 86–93, 2006.
- 634 Halofsky, J. E., Peterson, D. L., and Harvey, B. J.: Changing wildfire, changing forests: the
635 effects of climate change on fire regimes and vegetation in the Pacific Northwest, USA, *Fire
636 Ecology*, 16, 4, 2020.
- 637 Hatch, L. E., Jen, C. N., Kreisberg, N. M., Selimovic, V., Yokelson, R. J., Stamatis, C., York, R.
638 A., Foster, D., Stephens, S. L., Goldstein, A. H., and Barsanti, K. C.: Highly Speciated
639 Measurements of Terpenoids Emitted from Laboratory and Mixed-Conifer Forest Prescribed
640 Fires, *Environ. Sci. Technol.*, 53, 9418–9428, 2019.
- 641 Haugo, R. D., Kellogg, B. S., Cansler, C. A., Kolden, C. A., Kemp, K. B., Robertson, J. C.,
642 Metlen, K. L., Vaillant, N. M., and Restaino, C. M.: The missing fire: quantifying human
643 exclusion of wildfire in Pacific Northwest forests, USA, *Ecosphere*, 10, e02702, 2019.
- 644 Heyerdahl, E. K., Miller, R. F., and Parsons, R. A.: History of fire and Douglas-fir establishment
645 in a savanna and sagebrush–grassland mosaic, southwestern Montana, USA, *For. Ecol. Manage.*,
646 230, 107–118, 2006.
- 647 Jolly, W. M., Cochrane, M. A., Freeborn, P. H., Holden, Z. A., Brown, T. J., Williamson, G. J.,
648 and Bowman, D. M. J. S.: Climate-induced variations in global wildfire danger from 1979 to
649 2013, *Nat. Commun.*, 6, 7537, 2015.
- 650 Keeley, J. E.: Fire intensity, fire severity and burn severity: a brief review and suggested usage,
651 *Int. J. Wildland Fire*, 18, 116–126, 2009.
- 652 Kelly, S. D., Hesterberg, D., and Ravel, B.: Analysis of soils and minerals using X-ray
653 absorption spectroscopy, in: *Methods of Soil Analysis Part 5—Mineralogical Methods*,
654 American Society of Agronomy and Soil Science Society of America, Madison, WI, USA, 387–
655 463, 2015.
- 656 Kruse, J., Abraham, M., Amelung, W., Baum, C., Bol, R., Kühn, O., Lewandowski, H.,
657 Niederberger, J., Oelmann, Y., Rieger, C., Santner, J., Siebers, M., Siebers, N., Spohn, M.,



- 658 Vestergren, J., Vogts, A., and Leinweber, P.: Innovative methods in soil phosphorus research: A
659 review, *J. Plant Nutr. Soil Sci.*, 178, 43–88, 2015.
- 660 Lane, P. N. J., Sheridan, G. J., Noske, P. J., and Sherwin, C. B.: Phosphorus and nitrogen exports
661 from SE Australian forests following wildfire, *J. Hydrol.*, 361, 186–198, 2008.
- 662 Lenth, R. V.: emmeans: Estimated marginal means, Github,
663 <https://doi.org/10.1080/00031305.1980.10483031>, 2023.
- 664 Li, B. and Brett, M. T.: The influence of dissolved phosphorus molecular form on recalcitrance
665 and bioavailability, *Environ. Pollut.*, 182, 37–44, 2013.
- 666 Lopez, A. M., Avila, C. C. E., VanderRoest, J. P., Roth, H. K., Fendorf, S., and Borch, T.:
667 Molecular insights and impacts of wildfire-induced soil chemical changes, *Nature Reviews Earth
668 & Environment*, 5, 431–446, 2024.
- 669 Makarov, M. I., Haumaier, L., Zech, W., Marfenina, O. E., and Lysak, L. V.: Can ³¹P NMR
670 spectroscopy be used to indicate the origins of soil organic phosphates?, *Soil Biol. Biochem.*, 37,
671 15–25, 2005.
- 672 McDowell, R. W., Worth, W., and Carrick, S.: Evidence for the leaching of dissolved organic
673 phosphorus to depth, *Sci. Total Environ.*, 755, 142392, 2021.
- 674 McMeeking, G. R., Kreidenweis, S. M., Baker, S., Carrico, C. M., Chow, J. C., Collett, J. L., Jr,
675 Hao, W. M., Holden, A. S., Kirchstetter, T. W., Malm, W. C., Moosmüller, H., Sullivan, A. P.,
676 and Wold, C. E.: Emissions of trace gases and aerosols during the open combustion of biomass
677 in the laboratory, *J. Geophys. Res. D: Atmos.*, 114, <https://doi.org/10.1029/2009JD011836>,
678 2009.
- 679 Merino, A., Jiménez, E., Fernández, C., Fontúrbel, M. T., Campo, J., and Vega, J. A.: Soil
680 organic matter and phosphorus dynamics after low intensity prescribed burning in forests and
681 shrubland, *J. Environ. Manage.*, 234, 214–225, 2019.
- 682 Mishra, A., Alnahit, A., and Campbell, B.: Impact of land uses, drought, flood, wildfire, and
683 cascading events on water quality and microbial communities: A review and analysis, *J. Hydrol.*,
684 596, 125707, 2021.
- 685 Mukherjee, A. and Zimmerman, A. R.: Organic carbon and nutrient release from a range of
686 laboratory-produced biochars and biochar–soil mixtures, *Geoderma*, 193–194, 122–130, 2013.
- 687 Myers-Pigg, A. N., Grieger, S., Roebuck, J. A., Jr, Barnes, M. E., Bladon, K. D., Bailey, J. D.,
688 Barton, R., Chu, R. K., Graham, E. B., Homolka, K. K., Kew, W., Lipton, A. S., Scheibe, T.,
689 Toyoda, J. G., and Wagner, S.: Experimental Open Air Burning of Vegetation Enhances Organic
690 Matter Chemical Heterogeneity Compared to Laboratory Burns, *Environ. Sci. Technol.*, 58,
691 9679–9688, 2024.
- 692 Noack, S. R., McLaughlin, M. J., Smernik, R. J., McBeath, T. M., and Armstrong, R. D.: Crop
693 residue phosphorus: speciation and potential bio-availability, *Plant Soil*, 359, 375–385, 2012.



- 694 Parsons, A., Robichaud, P., Lewis, S. A., Napper, C., and Clark, J. T.: Field guide for mapping
695 post-fire soil burn severity, United States Department of Agriculture Forest Service Rocky
696 Mountain Research Station, <https://doi.org/10.2737/RMRS-GTR-243>, 2010.
- 697 R Core Team: R: A Language and Environment for Statistical Computing, 2023.
- 698 Randerson, J. T., Chen, Y., van der Werf, G. R., Rogers, B. M., and Morton, D. C.: Global
699 burned area and biomass burning emissions from small fires, *Biogeosciences*, 117,
700 <https://doi.org/10.1029/2012JG002128>, 2012.
- 701 Ravel, B. and Newville, M.: ATHENA, ARTEMIS, HEPHAESTUS: data analysis for X-ray
702 absorption spectroscopy using IFEFFIT, *J. Synchrotron Radiat.*, 12, 537–541, 2005.
- 703 Recena, R., Cade-Menun, B. J., and Delgado, A.: Organic phosphorus forms in agricultural soils
704 under Mediterranean climate, *Soil Sci. Soc. Am. J.*, 82, 783–795, 2018.
- 705 Reilly, M. J., Dunn, C. J., Meigs, G. W., Spies, T. A., Kennedy, R. E., Bailey, J. D., and Briggs,
706 K.: Contemporary patterns of fire extent and severity in forests of the Pacific Northwest, USA
707 (1985–2010), *Ecosphere*, 8, e01695, 2017.
- 708 Robinson, J. S., Baumann, K., Hu, Y., Hagemann, P., Kebelmann, L., and Leinweber, P.:
709 Phosphorus transformations in plant-based and bio-waste materials induced by pyrolysis, *Ambio*,
710 47, 73–82, 2018.
- 711 Roebuck, J. A., Jr, Grieger, S., Barnes, M. E., Gillespie, X., Bladon, K. D., Bailey, J. D.,
712 Graham, E. B., Chu, R., Kew, W., Scheibe, T. D., and Myers-Pigg, A. N.: Molecular shifts in
713 dissolved organic matter along a burn severity continuum for common land cover types in the
714 Pacific Northwest, USA, *Sci. Total Environ.*, 958, 178040, 2024.
- 715 Rose, T. J., Schefe, C., Weng, Z. (han), Rose, M. T., van Zwieten, L., Liu, L., and Rose, A. L.:
716 Phosphorus speciation and bioavailability in diverse biochars, *Plant Soil*, 443, 233–244, 2019.
- 717 Rust, A. J., Hogue, T. S., Saxe, S., and McCray, J.: Post-fire water-quality response in the
718 western United States, *Int. J. Wildland Fire*, 27, <https://doi.org/10.1071/WF17115>, 2018.
- 719 Saa, A., Trasar-Cepeda, M. C., Gil-Sotres, F., and Carballas, T.: Changes in soil phosphorus and
720 acid phosphatase activity immediately following forest fires, *Soil Biol. Biochem.*, 25, 1223–
721 1230, 1993.
- 722 Santín, C., Doerr, S. H., Merino, A., Bucheli, T. D., Bryant, R., Ascough, P., Gao, X., and
723 Masiello, C. A.: Carbon sequestration potential and physicochemical properties differ between
724 wildfire charcoals and slow-pyrolysis biochars, *Sci. Rep.*, 7, 11233, 2017.
- 725 Santín, C., Otero, X. L., Doerr, S. H., and Chafer, C. J.: Impact of a moderate/high-severity
726 prescribed eucalypt forest fire on soil phosphorous stocks and partitioning, *Sci. Total Environ.*,
727 621, 1103–1114, 2018.



- 728 Schaller, J., Tischer, A., Struyf, E., Bremer, M., Belmonte, D. U., and Potthast, K.: Fire enhances
729 phosphorus availability in topsoils depending on binding properties, *Ecology*, 96, 1598–1606,
730 2015.
- 731 Silber, A., Levkovitch, I., and Graber, E. R.: pH-dependent mineral release and surface
732 properties of cornstraw biochar: agronomic implications, *Environ. Sci. Technol.*, 44, 9318–9323,
733 2010.
- 734 Silins, U., Bladon, K. D., Kelly, E. N., Esch, E., Spence, J. R., Stone, M., Emelko, M. B., Boon,
735 S., Wagner, M. J., Williams, C. H. S., and Tichkowsky, I.: Five-year legacy of wildfire and
736 salvage logging impacts on nutrient runoff and aquatic plant, invertebrate, and fish productivity,
737 *Ecohydrol.*, 7, 1508–1523, 2014.
- 738 Smil, V.: PHOSPHORUS IN THE ENVIRONMENT: Natural Flows and Human Interferences,
739 *Annu. Rev. Environ. Resour.*, 25, 53–88, 2000.
- 740 Son, J.-H., Kim, S., and Carlson, K. H.: Effects of Wildfire on River Water Quality and Riverbed
741 Sediment Phosphorus, *Water Air Soil Pollut. Focus*, 26, 26, 2015.
- 742 Souza-Alonso, P., Prats, S. A., Merino, A., Guiomar, N., Guijarro, M., and Madrigal, J.: Fire
743 enhances changes in phosphorus (P) dynamics determining potential post-fire soil recovery in
744 Mediterranean woodlands, *Sci. Rep.*, 14, 21718, 2024.
- 745 Stavi, I.: Wildfires in Grasslands and Shrublands: A Review of Impacts on Vegetation, Soil,
746 Hydrology, and Geomorphology, *Water*, 11, 1042, 2019.
- 747 Strand, E. K., Bunting, S. C., and Keefe, R. F.: Influence of Wildland Fire Along a Successional
748 Gradient in Sagebrush Steppe and Western Juniper Woodlands, *Rangeland Ecol. Manage.*, 66,
749 667–679, 2013.
- 750 Sun, K., Qiu, M., Han, L., Jin, J., Wang, Z., Pan, Z., and Xing, B.: Speciation of phosphorus in
751 plant- and manure-derived biochars and its dissolution under various aqueous conditions, *Sci.*
752 *Total Environ.*, 634, 1300–1307, 2018.
- 753 Turner, B. L., Cade-Menun, B. J., and Westermann, D. T.: Organic Phosphorus Composition and
754 Potential Bioavailability in Semi-Arid Arable Soils of the Western United States, Published in
755 *Soil Sci. Soc. Am. J.*, 67, 1168–1179, 2003a.
- 756 Turner, B. L., Mahieu, N., and Condon, L. M.: Phosphorus-31 nuclear magnetic resonance
757 spectral assignments of phosphorus compounds in soil NaOH–EDTA extracts, *Soil Sci. Soc.*
758 *Am. J.*, 67, 497–510, 2003b.
- 759 Turrion, M.-B., Lafuente, F., Aroca, M.-J., López, O., Mulas, R., and Ruipérez, C.:
760 Characterization of soil phosphorus in a fire-affected forest Cambisol by chemical extractions
761 and ³¹P-NMR spectroscopy analysis, *Sci. Total Environ.*, 408, 3342–3348, 2010.



- 762 Uchimiya, M. and Hiradate, S.: Pyrolysis temperature-dependent changes in dissolved
763 phosphorus speciation of plant and manure biochars, *J. Agric. Food Chem.*, 62, 1802–1809,
764 2014.
- 765 Uchimiya, M., Hiradate, S., and Antal, M. J., Jr: Dissolved Phosphorus Speciation of Flash
766 Carbonization, Slow Pyrolysis, and Fast Pyrolysis Biochars, *ACS Sustainable Chem. Eng.*, 3,
767 1642–1649, 2015.
- 768 Method 365.3: Phosphorus, All Forms (Colorimetric, Ascorbic Acid, Two Reagent):
769 https://www.epa.gov/sites/default/files/2015-08/documents/method_365-3_1978.pdf.
- 770 Vega, J. A., Fontúrbel, T., Merino, A., Fernández, C., Ferreiro, A., and Jiménez, E.: Testing the
771 ability of visual indicators of soil burn severity to reflect changes in soil chemical and microbial
772 properties in pine forests and shrubland, *Plant Soil*, 369, 73–91, 2013.
- 773 Weihrauch, C. and Opp, C.: Ecologically relevant phosphorus pools in soils and their dynamics:
774 The story so far, *Geoderma*, 325, 183–194, 2018.
- 775 Werner, F. and Prietzel, J.: Standard Protocol and Quality Assessment of Soil Phosphorus
776 Speciation by P K-Edge XANES Spectroscopy, *Environ. Sci. Technol.*, 49, 10521–10528, 2015.
- 777 Wu, H., Yip, K., Kong, Z., Li, C.-Z., Liu, D., Yu, Y., and Gao, X.: Removal and Recycling of
778 Inherent Inorganic Nutrient Species in Mallee Biomass and Derived Biochars by Water
779 Leaching, *Ind. Eng. Chem. Res.*, 50, 12143–12151, 2011.
- 780 Wu, Y., Pae, L. M., Gu, C., and Huang, R.: Phosphorus Chemistry in Plant Ash: Examining the
781 Variation across Plant Species and Compartments, *ACS Earth Space Chem.*,
782 <https://doi.org/10.1021/acsearthspacechem.3c00145>, 2023a.
- 783 Wu, Y., Pae, L. M., and Huang, R.: Phosphorus chemistry in plant charcoal: interplay between
784 biomass composition and thermal condition, *Int. J. Wildland Fire*, 33, NULL-NULL, 2023b.
- 785 Xu, G., Zhang, Y., Shao, H., and Sun, J.: Pyrolysis temperature affects phosphorus
786 transformation in biochar: Chemical fractionation and ³¹P NMR analysis, *Sci. Total Environ.*,
787 569–570, 65–72, 2016.
- 788 Yan, Y., Wan, B., Jiang, R., Wang, X., Wang, H., Lan, S., Zhang, Q., and Feng, X.: Interactions
789 of organic phosphorus with soil minerals and the associated environmental impacts: A review,
790 *Pedosphere*, 33, 74–92, 2023.
- 791 Yu, F., Wang, J., Wang, X., Wang, Y., Guo, Q., Wang, Z., Cui, X., Hu, Y., Yan, B., and Chen,
792 G.: Phosphorus-enriched biochar from biogas residue of *Eichhornia crassipes*: transformation
793 and release of phosphorus, *Biochar*, 5, 82, 2023.
- 794 Yusiharni, E. and Gilkes, R.: Minerals in the ash of Australian native plants, *Geoderma*, 189–
795 190, 369–380, 2012.



- 796 Zavala, L. M., De Celis, R., and Jordán, A.: How wildfires affect soil properties. A brief review,
797 Cuad. Investig. Geogr., 40, 311–332, 2014.
- 798 Zheng, H., Wang, Z., Deng, X., Zhao, J., Luo, Y., Novak, J., Herbert, S., and Xing, B.:
799 Characteristics and nutrient values of biochars produced from giant reed at different
800 temperatures, Bioresour. Technol., 130, 463–471, 2013.
- 801 Zwetsloot, M. J., Lehmann, J., and Solomon, D.: Recycling slaughterhouse waste into fertilizer:
802 how do pyrolysis temperature and biomass additions affect phosphorus availability and
803 chemistry?, J. Sci. Food Agric., 95, 281–288, 2015.